National Conference with International Participation
ENGINEERING MECHANICS 2006
Svratka, Czech Republic, May 15 – 18, 2006
paper no. 200

EFFECT OF CREEP IN EVALUATION OF NANOINDENTATION OF CEMENT PASTES

J. Němeček*, P. Kabele*, P. Jůn*

Summary: *This paper deals with nanoindentation of cement paste as a representative of heterogeneous and time-dependent building material. The paper concerns on the appropriateness of methods used for evaluation of micromechanical properties. Limitation of traditional elastic solution is shown on the unique experimental program. Better descriptions of indentation process based on analytical viscoelastic solution and finite element model with general viscoelastoplastic constitutive relation are proposed. These models are used for simulation of indentation and for estimation of material parameters at micrometer scale.*

1. Introduction

It is a doubtless fact that the overall material behavior is directly dependent on the microstructure and its individual phase properties. Modern constitutive models for composite materials try to respect this fact and link the overall material response with its microlevel. It can be done using multiscale approach that upscales these properties from microlevel to the engineering macroscale properties. The development of various experimental techniques in the past decades made possible to access mechanical properties of various materials at submicron length scales. Nanoindentation plays an important role among the new experimental techniques. This technique is based on the direct measurement of the load-displacement relationship using a very sharp diamond tip pressed into the material. The depth of penetration starts from the level of nanometers. Although, nanoindentation was originally developed and used mainly for studying homogeneous materials like metals, coatings, films, glass, and crystal materials, the evolution of this method allows us to use it also for materials like concrete and cement. The major studies can be found e.g. in Constantinides, Ulm and Van Vliet (2003), Constantinides and Ulm (2004), Velez et al. (2001). However, the interpretation of measured data is more complicated due to the large heterogeneity of concrete and cement as well.

In contrary to classical macroscopic tests, numerous microscale phenomena can occur during indentation tests. Size-dependent indentation results are commonly obtained and reported mainly for metals by many researchers Choi et al. (2003), Wei et al. (2004), Elmustafa and Stone (2002). Creep of the material was found to be the main factor contributing to such interpretations. Ignoring creep in the evaluation of results can lead to overestimation of size effect on hardness and spurious size effect on elastic properties.

* ing. Jiří Němeček, Ph.D., doc. ing. Petr Kabele, Ph.D., ing. Petr Jůn: ČVUT v Praze, Fakulta stavební, Katedra mechaniky, Thákurova 7, 16629 Praha 6, tel. +420224354309, fax +420224310775, e-mail: jiri.nemecek@fsv.cvut.cz

Simulation of indentation process and comparison with experimental data can answer the question on the appropriateness of different constitutive relations and the underlying material behavior.

2. Nanoindentation of cement pastes

Cement paste is a very specific and important part of building materials. Although cementitious matrix is a heterogeneous material it can be treated as homogeneous in a micrometer length scale. The major constituents are hydrated phases (C-S-H gels, Portlandite), unhydrous phases (rest of clinkers) and porosity. Nanoindentation can be employed for assessment of micromechanical properties of these individual phases in the way that a large number of indents is produced and subsequently separated into specific phase groups. Since the scatter of results is commonly much higher than for metal materials, for instance, the results are treated in the statistical way.

An example of indented cement paste sample, which is usually produced in a rectangular area, is shown in Fig. 1. Typical pyramidal shape of indenter imprints is formed by the shape of Berkowich indenter tip. Micromechanical properties can be evaluated for each indent in the matrix. Separation of indents in to phase groups is done with the aid of electron microscope (ESEM).

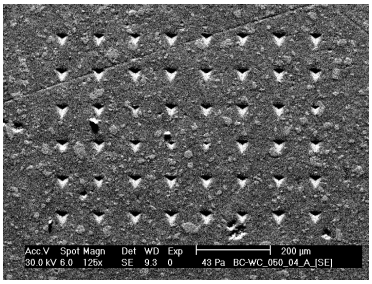

Fig. 1 ESEM image of indented cement paste- matrix with large indents (5500 nm in depth).

3. Evaluation of nanoindentation results

Experimental results from nanoindentation cover the load vs. depth of penetration diagram (the P-h curve). This diagram contains loading and unloading branch and may contain also holding (dwelling) period at the peak of the diagram (Fig. 2).

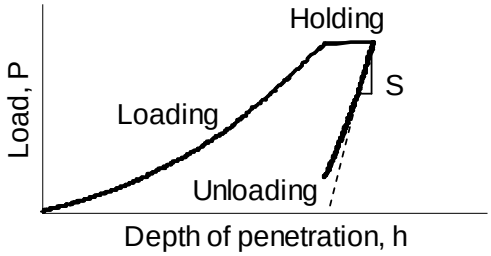

Fig. 2 Nanoindentation load vs. depth of penetration diagram (P-h curve).

Traditionally, only elastic properties such as elastic modulus and hardness are evaluated from the unloading branch. The method for interpreting nanoindentation results is of crucial importance to evaluation of micromechanical properties. Several methods have been proposed

in the past. One of the favorite methods is authored by Oliver and Pharr (1992). The method is based on the assumption of indentation in a homogeneous body modeled as an isotropic elastic half-space. In such case, the solution is known in analytical form and experimentally measured contact stiffness can be used for an inverse analysis of material parameters. However, there are still many open questions concerning the indentation process itself and the subsequent evaluation of the material properties especially for time-dependent materials like cement paste.

A variety of reasons are responsible for complicated material behavior and misinterpretations of experimental data at the microscale. The most important are: specimen preparation, oxidation of surface, surface roughness, assessment of contact area under indenter, development of dislocations in the specimen body and last but not least effects of loading time and associated material creep. Since the first series of reasons can be minimized in most cases, the later reason cannot be fully avoided and thus it was studied in large extent in this paper.

4. Experimental results

White cement paste samples (CEM-I 52,5 White, Holcim, SK) mixed in water/cement ratio w/c=0.5 were prepared and stored in water for 28 days. Before testing, a 2 mm thick slice from the bulk material was cut and polished on coarse to very fine emery papers to achieve very smooth and flat surface, e.g. Detwiler (2001). Specimens were washed in ultrasonic bath to remove all the dust. The resultant surface had the roughness about several tens of nm as checked by AFM.

To study creep effects two different series of specimens were tested. The first series “O” was tested without holding period at the peak. Long holding period was applied for the second series “C”. Both series were tested in several load levels in the range of 2-300 mN.

It can be seen in Fig. 3a that the P-h curve contains a “bulge” or “nose” at the beginning of unloading in each cycle. It shows the role of creep that is present even on the unloading branch. As a consequence of this finding the assumptions of elastic solution are not fulfilled and evaluation of results leads to spurious size effect on elastic properties as discussed later.

5. Analysis of indentation data and their numerical simulation

5.1 Elastic solution

Commonly, two elastic properties, the hardness and the elastic modulus are extracted from indentation data. The most popular method was elaborated by Oliver and Pharr. The elastic properties are evaluated from an unloading part of the P-h curve. The analysis is based on the analytical solution known for rotational bodies punched into the elastic isotropic half-space.

Hardness and indentation modulus are than defined as follows:

$$H = \frac{P_{\max}}{A} \tag{1}$$

$$E_r = \frac{S\sqrt{\pi}}{2\sqrt{A}} \tag{2}$$

where P_{max} is the peak load, A is the projected contact area at peak load and S is the contact stiffness evaluated as the initial slope of unloading curve (Fig. 2). The effect of non-rigid indenter can be accounted for by the following equation:

$$\frac{1}{E_r} = \frac{1-\nu^2}{E} + \frac{1-\nu_i^2}{E_i} \tag{3}$$

where E and ν are tested material elastic modulus and Poisson's ratio, respectively. E_i and ν_i are indenter's parameters (for diamond: E_i=1141 GPa and ν_i =0.07).

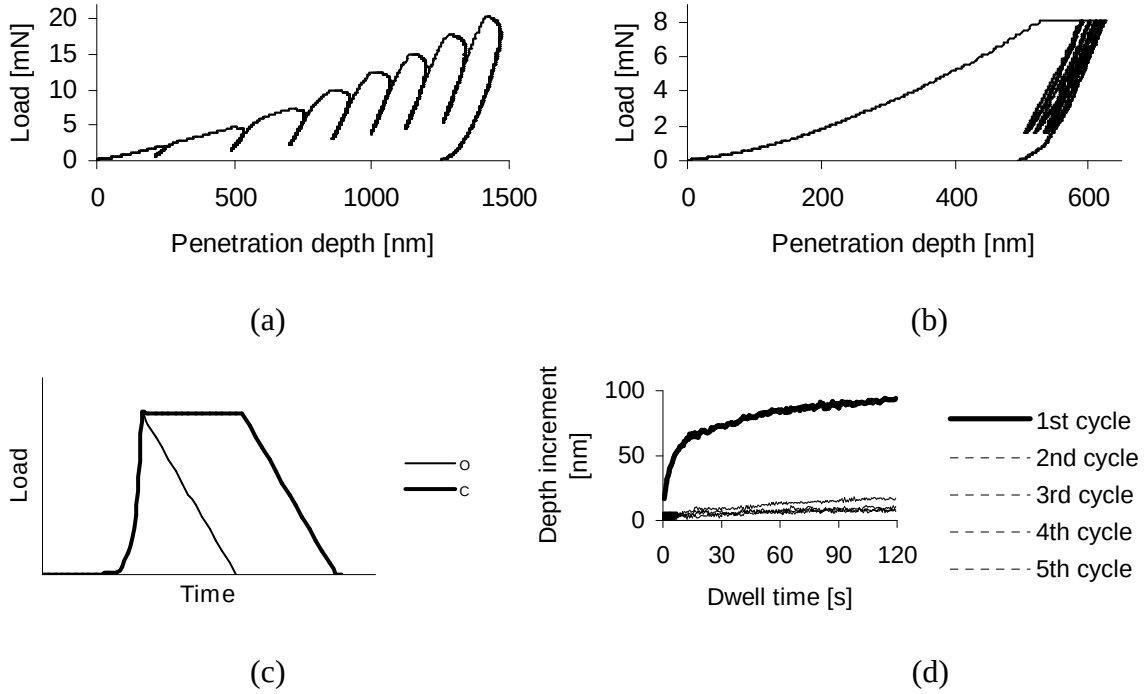

Fig. 3. Experimental results- examples of indentation load-depth diagrams.
(a) Series "O"- multiple loading cycles with increasing load (subrange 2-20 mN) with no dwell period at the peak.
(b) Series "C"- 5 loading/unloading cycles to the same load (8 mN) with dwell period at the peak 120 s.
(c) Time course of loading process of a single cycle: exponential loading to the peak, dwell period (only "C" series) and linear unloading.
(d) example of indentation creep during the 120 s dwell period at the peak of loading diagram (series "C") for the load level 8 mN.

5.2 Viscoelastic solution

According to experimental evidence cement paste is a time-dependent material whose behavior cannot be characterized only by elasticity. Elastic modulus can be extracted from P-h curve in case of a special loading with long dwell periods and cyclic loading ("C" series) where the effect of creep on the unloading branch is minimized. However, simulation of the indentation process cannot be achieved. Several models can be proposed to solve such phenomena. Recent work of Vandamme and Ulm (2005) assumes that the indentation

response is dominated by viscoelastic behavior. Multiple formulations can be constructed in such case. Vandamme and Ulm derived closed form analytical solution based on the assumption of linear viscoelastic material with deviator creep. The best results are obtained using 5-parameter combined Kelvin-Voigt-Maxwell model as shown in Fig. 4. Viscous deformation in this model is given by

$$G_0 n_v n_M 2\ddot{\varepsilon}_d(t) + G_0 G_v n_M 2\dot{\varepsilon}_d(t) = \\ = n_v n_M \ddot{\sigma}_d(t) + (G_0 n_v + G_0 n_M + G_v n_M)\dot{\sigma}_d(t) + G_0 G_v \sigma_d(t) \quad (4)$$

where ε_d and σ_d are deviator part of strain and stress tensor, respectivelly. Dots over the tensors have the meaning of time derivatives. G_0 and G_v are elastic stiffness parameters, n_m and n_v are viscosity parameters as also can be seen in Fig. 4.

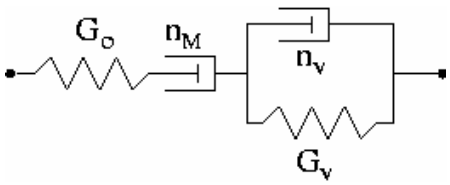

Fig. 4 Schematic representation of 5-parameter linear viscoelastic deviator creep model based on combined Kelvin-Voigt-Maxwell chain.

For a specific load-time function an analytical solution was derived for loading and holding periods. Unloading cannot in general be described by this solution since the derivation of the analytical form was based on the assumption of monotonically increasing contact area that is not the case of unloading. Viscoelastic model parameters can be obtained by nonlinear fitting of the experimental data from holding period where the force is kept constant over the time.

5.3 Finite element analysis

It follows from the previous paragraphs, that analytical solutions of the indentation problem are presently available only for some simple constitutive models and special loading histories. It also appears that neither the elastic, nor the viscoelastic model fully represent the behavior of cement paste. Therefore, performance of more complex material models was examined in conjunction with the finite element (FE) method.

The employed constitutive model utilizes the decomposition of the strain tensor:

$$\varepsilon_{ij} = \varepsilon_{ij}^E + \varepsilon_{ij}^C + \varepsilon_{ij}^P \quad (5)$$

where ε_{ij}^E is the time-independent and fully recoverable elastic component of strain, ε_{ij}^C is the time-dependent viscous component of strain (creep strain), and ε_{ij}^P is time-independent plastic strain. The elastic strain is related to stress through isotropic elastic compliance tensor.

The evolution of creep strain is governed by a creep flow rule:

$$\dot{\varepsilon}_{ij}^C = \gamma \frac{\partial J_2}{\partial \sigma_{ij}} \quad (6)$$

where a dot symbol above indicates time rate and J_2 is the creep potential expressed by the second invariant of deviatoric stress tensor. Scalar γ depends on the current value of equivalent stress

$$\bar{\sigma} = \left(3J_2\right)^{\frac{1}{2}} \tag{7}$$

and the equivalent creep strain, which is expressed by the power creep law:

$$\bar{\varepsilon}^C = a_0 \bar{\sigma}^{a_1} t^{a_2} \tag{8}$$

Here a_0, a_1, a_2 are material constants and t stands for time.

In contrary to creep strains, plastic strains develop only upon satisfaction of the von Mises yield condition

$$J_2 - \frac{1}{3}\sigma_Y = 0 \tag{9}$$

where σ_Y is a material parameter (uniaxial yield strength). The evolution of plastic strain then follows the associated flow rule and perfect plasticity.

In general, the constitutive model is characterized by two elastic parameters (E, ν), three creep parameters (a_0, a_1, a_2) and one plastic parameter (σ_Y).

The geometry of the nanoindentation experiments was simplified in FE model by assuming axial symmetry of both the indenter and the material specimen. The height of the modeled domain was equal to that of the real specimen (4 mm), while the diameter was reduced to one half (15 mm – which is still much larger than the zone affected by any indent). The FE mesh consisted of 1800 isoparametric four-node elements and it was significantly refined in the proximity of the indent (Fig. 5). The indenter was modeled as perfectly rigid and its variable contact with the specimen was identified and imposed in each loading step. The analysis was performed with consideration of large strains and large displacement.

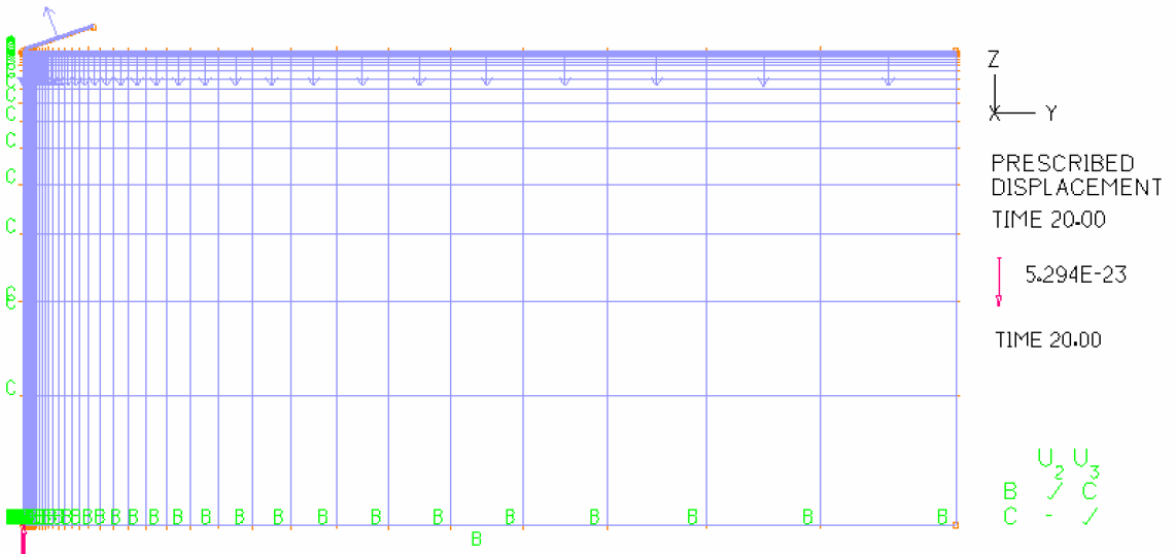

Fig. 5 Finite element mesh and boundary conditions

6. Results and discussion

First the experimental data were evaluated according to standard Oliver-Pharr methodology (i.e. assuming elastic behavior at the unloading and ignoring creep effects). It was found it leads to spurious size effect on elastic modulus as well as hardness. It is caused by the presence of creep in the initial part of the unloading branch of P-h curve ("bulge") as can be seen in case of "O" samples (Fig. 3a). In case of using long dwell period in the combination with cyclic loading this size effect was minimized on elastic modulus (Fig. 6b). Hardness is still influenced since different loading paths lead to different contact areas in Eq. 1 and consequently it leads to size effect on H even for "C" samples.

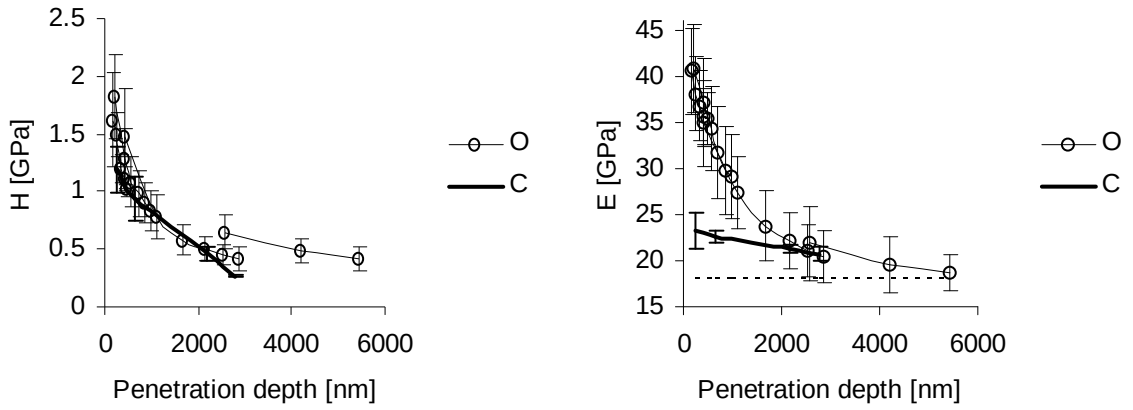

(a) (b)

Fig. 6 (a) Hardness and (b) elastic modulus evaluated for hydrated cement paste. "O" stands for series with increasing loading cycles without dwell period at peak, "C" stands for series tested by cyclic loading to the same load with 120 s dwell period at the peak. Dotted line represents macroscopic limit measured on full-scale specimens.

Second, analytical viscolelastic solution was applied to the simulation of some experimental P-h curves. Material parameters were obtained by nonlinear least-square fitting (standard nonlinear Levenberg-Marquardt procedure solved in software Matlab) of material creep during holding period (Fig. 7a). Such set of parameters was used for simulation of the loading curve. The results are quite satisfactory as can be seen in Fig. 7b.

The same procedure was applied for more complex type of experiment with cyclic loading (Fig. 7c). Since the loading path was too complicated for the analytical solution simplified loading history without intermediate unloading was used. It is the reason why no cyclic loading is obtained in the simulation in Fig. 7c. However the numerical response does not wrap the experimental curve as it was expected. Using the same material parameters lead to underestimation of deformation in this experiment. It motivated us to construct the FE model with more complex constitutive laws and with the possibility of setting an arbitrary loading history.

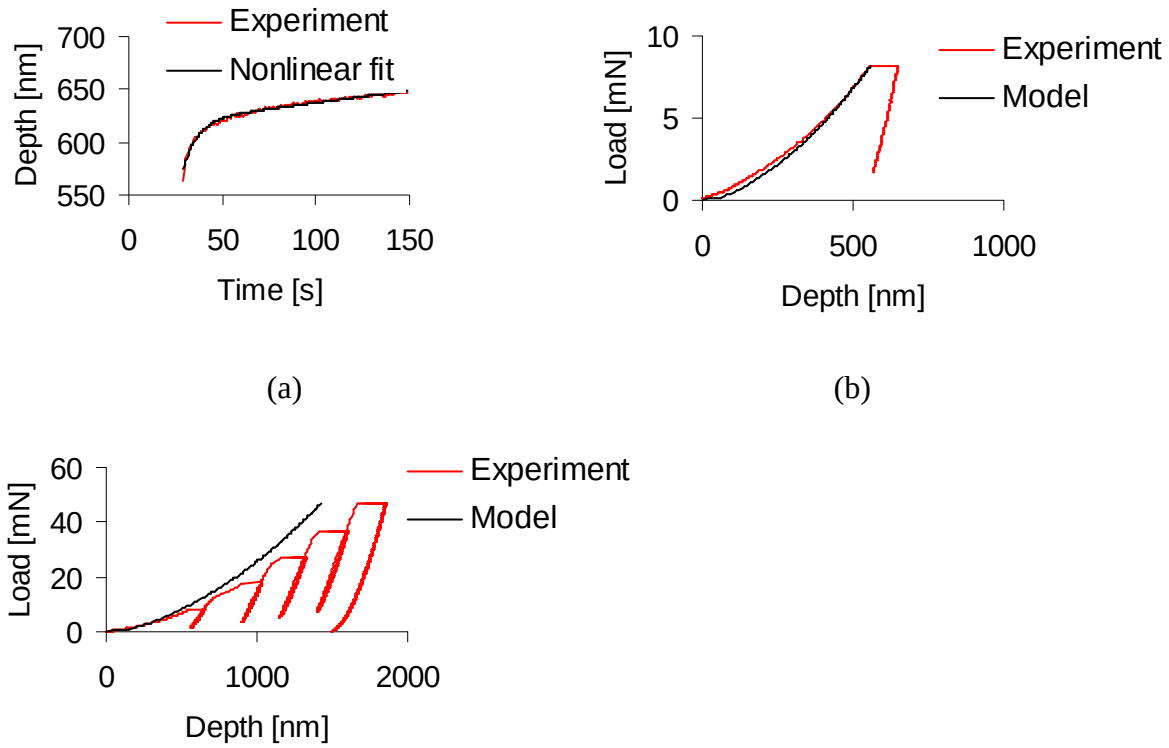

Fig. 7 Comparison of experimental results with viscoelastic solution. (a) Fitting of material parameters from creep in the holding period resulted in G_0=10.48 GPa, G_v=5.53 GPa, n_m=3870 GPa.s and n_v =43.7 GPa.s. (b) Simulation of loading curve. (c) Simulation of loading curve with cyclic loading.

In order to clarify the influence of different mechanisms of deformation on the response of cement paste in nanoindentation experiments, FE analyses were carried out with some or none of the strain components in Eq. 5 assumed equal to zero. In all calculations, the time history of applied indentation force earlier referred to as C-series was used (maximum force 50 mN, attained in five equal steps).

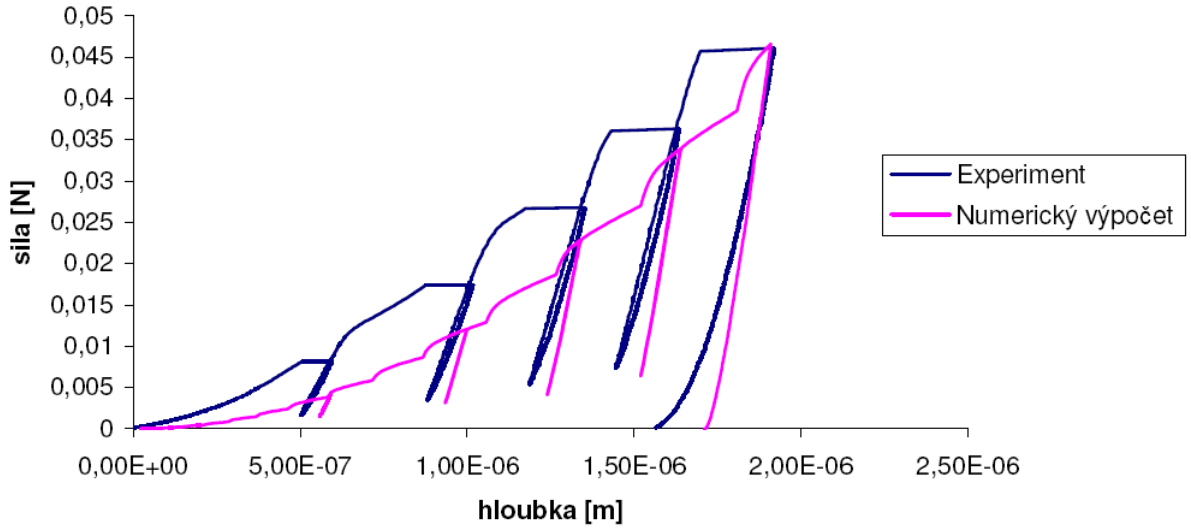

Fig. 8 Force vs. depth diagram for elastic-plastic material

Fig. 8 compares the experimental result and the response calculated with elastic perfectly-plastic material model. In this case, the material parameters (E = 23.25 GPa and σ_Y = 170 MPa) were determined so as to match the maximum force at maximum depth in the experiment. It is obvious from the figure, that due to excluding the viscous effects, the model cannot capture the creep of the material during load-dwell periods. The model also does not produce any hysteresis, which is typical for the unloading-reloading periods of the experiment.

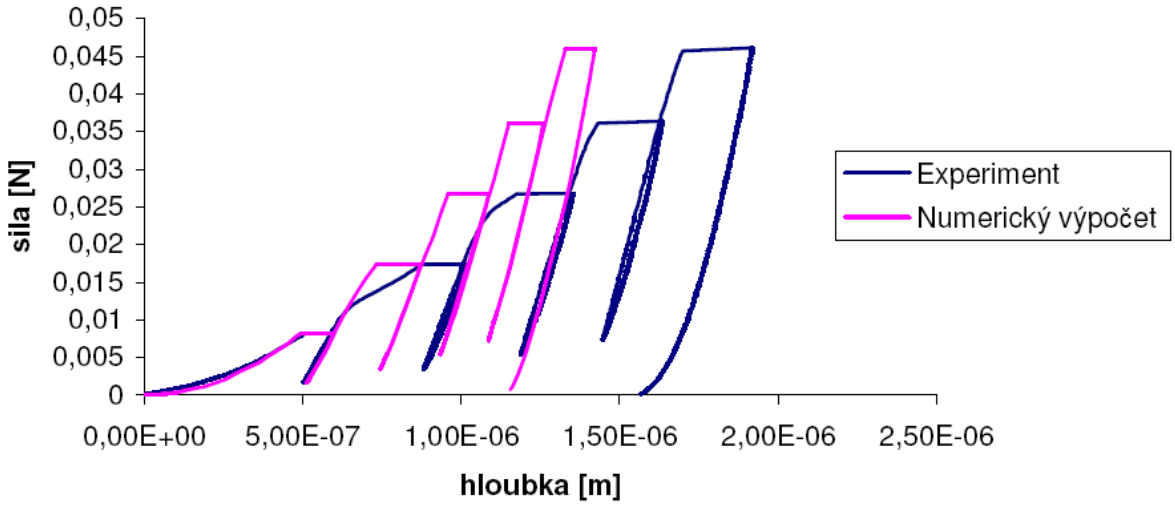

Fig. 9 Force vs. depth diagram for elastic-creep material

In another numerical experiment, we excluded plastic strains while creep strains were accounted for. The results are shown in Fig. 9. It is seen that even though material parameters were determined so as to fit well the first loading-dwell-unloading cycle, the subsequent cycles do not match. In particular, the model does not capture the significant reduction of tangential stiffness that occurs during loading periods of second, third, and fourth cycle.

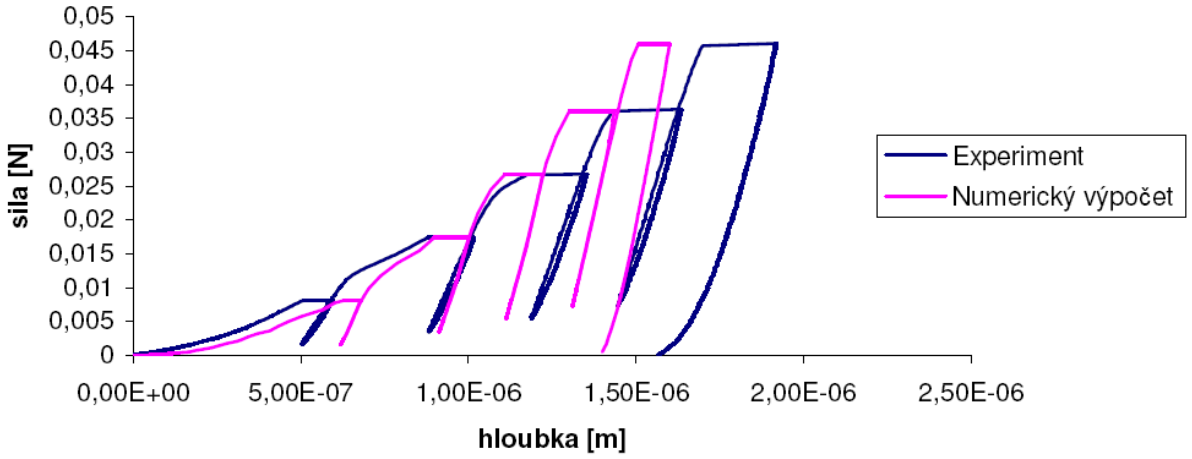

Fig. 10 Force vs. depth diagram for elastic-plastic-creep material

The model used for the last analysis included all strain components according to Eq. 5. In this case, the number of parameters was too high to be determined by a simple trial and error approach. The main difficulty consisted in the fact, that even during the dwell periods when the loading force was constant, creeping of the material under the indenter resulted in changing contact area and consequently in changing stress field. Thus, it was not possible to separate the response due to plastic yielding and creeping. However, Fig. 10 shows that this model qualitatively matches all the major features of the experimental response curve: the creep during load-dwell periods as well as variation of tangential stiffness during the loading phases. FE model also gives information on the deformations and stress field under the indenter probe as shown in Fig. 11.

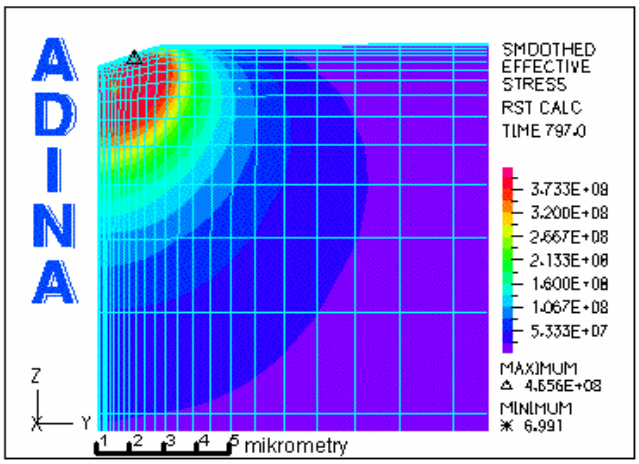

Fig. 11 FE model. Effective stress under indenter probe.

7. Concluding remarks

The presented work concerned on the evaluation of nanoindentation experiments measured on cement pastes. Since the traditional approaches based on elastic solution are not adequate for the simulation of cement paste more complex models are needed. The comparison of several approaches showed that classical elastic solution (Oliver and Pharr, 1992) can be used for the estimate of elastic parameters only in connection with a special loading path. A simple viscoelastic solution (Vandamme and Ulm, 2005) can capture the loading and holding periods of the P-h curve for one cycle experiment. However, using of the same material parameters does not lead to satisfactory results for the case of cyclic loading. Thus, a more general FE model was proposed. The FE analyses showed that in description of the micromechanical behavior of cement paste, both time-independent plastic strains and time-dependent creep stains appear to play an important role. However, parameters of the qualitatively most suitable elastic-plastic-creep model are difficult to obtain. Presently, the possibility of using a more sophisticated method of parameter identification based on genetic algorithms is being researched.

8. Acknowledgements

This work has been supported by the Ministry of Education of the Czech Republic (project MSM 6840770003) and Czech Grant Agency (GACR 103/05/0896). Their support is gratefully acknowledged.

9. References

Constantinides, G., Ulm F.J., Van Vliet K. (2003) 'On the use of nanoindentation for cementitious materials', Materials and Structures, 36, 191-196.

Constantinides, G., Ulm F.J. (2004) 'The effect of two types of C-S-H on the elasticity of cement-based materials: Results from nanoindentation and micromechanical modeling', Cement and Concrete Research, 34 (1), 67-80.

Choi Y., Van Vliet K.J., Li J., Suresh S. (2003) 'Size effect on the onset of plastic deformation during nanoindentation of thin films and patterned lines', Journal of Applied Physics, 94 (9).

Detwiler R.J. et al. (2001) 'Preparing Specimens for Microscopy', Concrete International 23 (11).

Elmustafa A.A., Stone D.S. (2002) 'Indentation size effect in polycrystalline F.C.C. metals', Acta Materialia 50 (14), 3641-3650.

Oliver W.C, Pharr G.M. (1992) 'An improved technique for determining hardness and elastic modulus using load and displacement sensing indentation experiments', Journal of Material Research 7, 1564-1583.

Vandamme M., Ulm F.J. (2005) 'Viscoelastic solutions for conical indentation', Int. J. of Solids and Structures, in press.

Velez K, et al. (2001) 'Determination of nanoindentation of elastic modulus and hardness of pure constituents of Portland cement clinker', Cement and Concrete Research 31, 555-561.

Wei, Y., Wang, X., Zhao, M. (2004) 'Size effect measurement and characterization in nanoindentation test', Journal of Material Research 19 (1), 208-217.